

기계적인 합금화에 의한 Mg-18wt.%Ni 수소저장합금의 개발

송명엽 · 안동수 · 권익현 · 안효준*

전북대학교 신소재공학부

*경상대학교 금속재료공학과

Development of Mg-18wt.%Ni Hydrogen-Storage Alloy by Mechanical Alloying

MyoungYoup Song, DongSu Ahn, IkHyun Kwon and HyoJun Ahn*

Division of New-Materials Engineering, Automobile High Technology Research Institute of Industrial Technology,
Chonbuk National University, 664-14 1 ga Deogjindong Deogjingu Chonju Chonbuk, 561-756

*Department of Metallurgical and Materials Engineering, Gyeongsang National University, 900 gazwadong Chinju Gyeongnam, 600-701

(1999년 9월 18일 받음, 1999년 11월 10일 최종수정본 받음)

초 록 기계적으로 합금처리한 Mg-18wt.%Ni 혼합물의 수소저장특성이 조사되었다. 1h, 3h, 그리고 6h 동안 기계적으로 합금처리한 혼합물들 중에서 6h동안 기계적으로 합금처리한 혼합물(MA 6h sample)이 가장 좋은 활성화, 수소화물 형성·분해 특성을 보인다. 수소화물 형성·분해 cycling을 시킴에 따라 Mg₂Ni 상이 형성된다. MA 6h sample은 비교적 쉽게 활성화되며, 순수한 Mg나 Mg-10wt.%Ni 합금보다 수소화물 형성속도가 높으나, Mg₂Ni 합금보다는 수소화물 형성속도가 약간 낮다. MA 6h sample은 Mg₂Ni 합금에 비해 낮은 수소화물 분해속도를 보이지만, 순수한 Mg나 Mg-25wt.%Ni 합금보다는 높은 수소화물 분해속도를 보인다. MA 6h sample은 순수한 Mg나 다른 합금들보다 큰 수소저장용량을 가지고 있다.

Abstract The hydrogen-storage properties of a mechanically-alloyed Mg-18wt.%Ni mixture were investigated. Among the mixtures mechanically alloyed for 1h, 3h, and 6h, the mixture mechanically alloyed for 6h (MA 6h sample) shows the best properties of activation, hydriding, and dehydriding. The Mg₂Ni phase forms in the mechanically-alloyed Mg-18wt.%Ni mixture along with hydriding-dehydriding cycling. The MA 6h sample is relatively easily activated and has higher hydriding rate than the pure Mg, the Mg-10wt.%Ni alloy, and a little lower hydriding rate than the Mg₂Ni alloy. The MA 6h sample shows lower dehydriding rate than the Mg₂Ni alloy but higher dehydriding rate than the pure Mg and the Mg-25wt.%Ni alloy. The MA 6h sample has larger hydrogen-storage capacity than the pure Mg and the other alloys.

Key words: Mg-18wt.%Ni hydrogen-storage alloy, mechanical alloying, Mg₂Ni, activation, hydriding and dehydriding rates.

1. Introduction

Magnesium has many advantages for a hydrogen storage material; large hydrogen storage capacity (7.6wt%), low cost and abundance in the Earth's crust. But its hydriding and dehydriding kinetics are very slow.¹⁾ Much work to ameliorate the reaction kinetics of magnesium with hydrogen has been carried out by alloying certain metals with magnesium,^{2~9)} by mixing metal additives with magnesium,¹⁰⁾ by plating nickel on the surface of magnesium¹¹⁾ and by synthesizing magnesium hydride in the presence of a homogeneous catalyst.¹²⁾ In particular, the Mg/Ni-H₂ system has been studied by alloying^{3,13~16)} and by plating.¹¹⁾

In this work we tried to improve the reaction kinetics of magnesium with hydrogen by mechanical alloying of magnesium with nickel. Among the alloys of Mg with Ni, the alloys Mg-10wt.%Ni and Mg-25wt.%Ni had

relatively good hydriding or dehydriding characteristics,^{4,17)} so we selected, for mechanical alloying of Mg with Ni, the composition Mg-18wt.%Ni which is the middle composition of the alloys Mg-10wt.%Ni and Mg-25wt.%Ni. The hydriding and dehydriding properties of a mechanically-alloyed mixture with a composition Mg-18wt.%Ni were investigated and they were compared with the hydrogen-storage properties of the Mg-10wt.%Ni alloy, the Mg-25wt.%Ni alloy, the pure Mg and the Mg₂Ni alloy.

2. Experimental details

Mechanical alloying of Mg with Ni in the composition Mg-18wt.%Ni was carried out in an attritor (high-energy ball mill) under argon atmosphere for 1h, 3h, and 6h. The weight ratio of sample to balls was 1/50. The purities of Mg, Ni powders were 99 and 99.5% respectively. The speed of the stirrer was 300rpm.

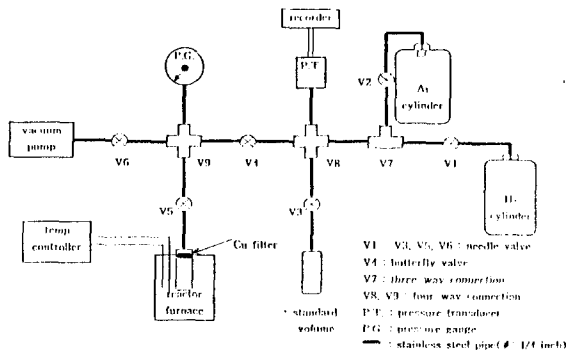


Fig. 1. Scheme of the hydriding and dehydriding apparatus.

Fig. 1. shows schematically the Sievert's type hydriding and dehydriding apparatus made of stainless-steel pipe. This apparatus consists of three parts ; gas (H_2 , Ar)cylinders, standard volume and reactor. Ar gas is used for measuring the dead volume of each part and for controlling the atmosphere during heating the reactor to reaction temperatures. The pressures in the standard volume and the reactor are read by a pressure gauge (P.G.) and a pressure transducer (P.T.) connected to the strip-chart recorder, respectively. The dead volume of the part for the standard volume with the pressure transducer is 297.0cm^3 , and that of the part for the reactor with the pressure gauge is 31.8cm^3 . A Cu-filter (made by sintering Cu powder) is inserted in the head of the reactor in order to prevent the sample powder from being pumped out during the operation of vacuum pump. The hydrogen pressures were maintained nearly constant during the hydriding and dehydriding reactions by dosing or taking out an appropriate quantity of hydrogen with a butterfly valve V_4 . The variation of the hydrogen pressure in the part of the standard volume permits one to calculate the quantity of hydrogen absorbed or desorbed by the sample as a function of time.

The phases in the mixtures hydrided before and after hydriding-dehydriding cycling were identified by X-ray ($\text{CuK}\alpha$) diffraction analysis.

The microstructures of the mixtures before and after hydriding-dehydriding cycling were observed by scanning electron microscope (SEM).

3. Results and discussions

We call the Mg-18wt.%Ni samples prepared by mechanical alloying for 1h, 3h, and 6h, MA 1h sample, MA 3h sample, and MA 6h sample respectively.

Fig. 2. shows the X-ray ($\text{CuK}\alpha$) powder diffraction patterns of MA 1h sample, MA 3h sample, MA 6h sam-

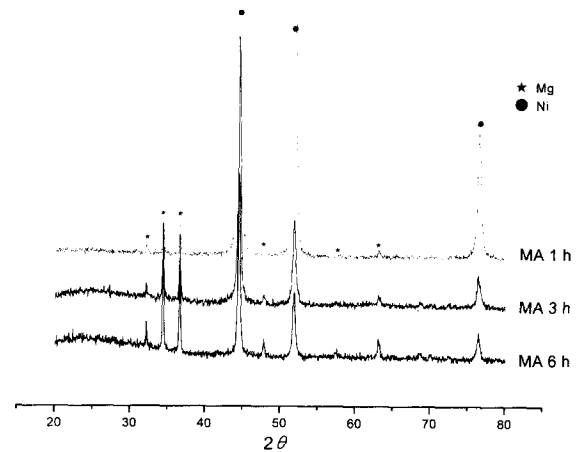


Fig. 2. X-ray diffraction patterns of (a) MA 1h, (a) MA 3h, (a) MA 6h samples as prepared.

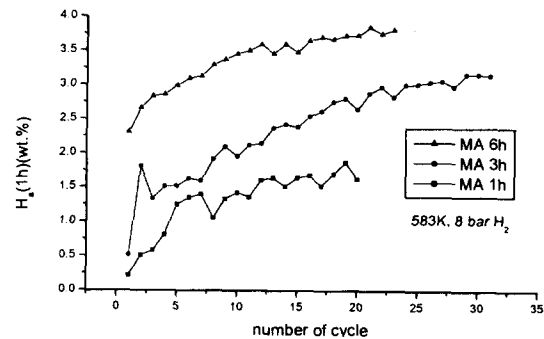


Fig. 3. Variations, with the number of cycle n , of the hydrogen absorbed for 1h $H_a(1h)$ by Mg-18wt.%Ni mechanically alloyed for three different times.

ple. The samples contain Mg and Ni. The intensities of the diffraction lines for Ni become weaker and the fluctuation of the background for the diffraction pattern becomes larger as the mechanical alloying time increases. These indicate that the sample becomes more amorphous with the increase in the mechanical alloying time.

H_a is defined as the weight percentage of absorbed hydrogen with respect to the sample weight.

Fig. 3. gives the variation, with the number of hydriding cycle, of the H_a during 1h, $H_a(1h)$, at 583K, 8bar H_2 for three samples mechanically alloyed for different times. The weights of the MA 1h, MA 3h, MA 6h samples used are 1g. At the first cycle the MA 6h sample has the largest value of $H_a(1h)$. The number of cycle, after which the value of $H_a(1h)$ remains constant or decreases, is about 19, 29, and 21 respectively. It is considered that the activations of the three samples are completed after these numbers of cycle. The MA 6h sample has the largest $H_a(1h)$ values at the first cycle and after activation : 2.31wt.% at the first cycle and

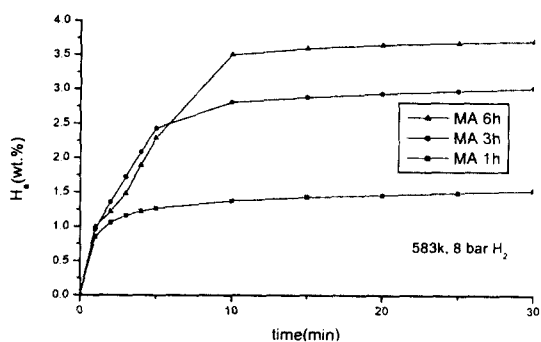


Fig. 4. H_a vs. t curves for three samples after activation.

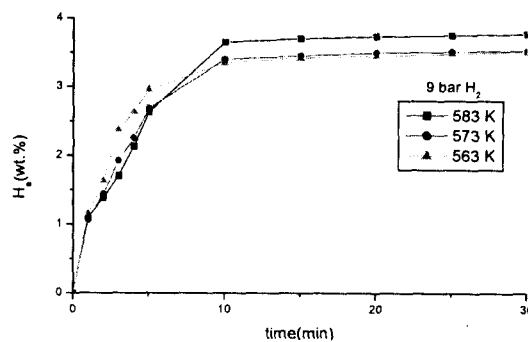


Fig. 6. H_a vs. t curves for the MA 6h sample under 9 bar H_2 at different temperatures.

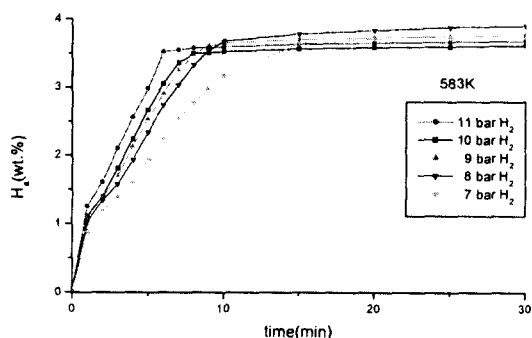


Fig. 5. H_a vs. t curves at 583 K for the MA 6h sample under different hydrogen pressures.

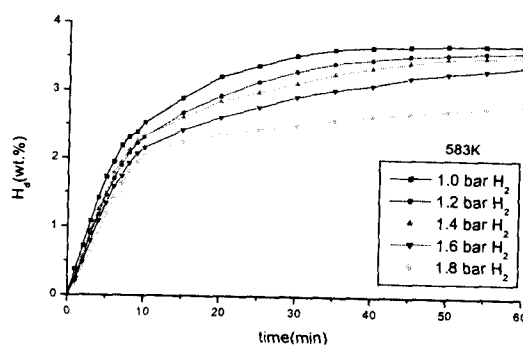


Fig. 7. Variations of the desorbed hydrogen H_d with time t at 583 K under different hydrogen pressures for the MA 6h sample.

3.85wt.% (at $n = 21$) after activation. The sudden decreases at certain numbers of cycle are probably due to the increase in the particle size due to coalescence caused by staying for relatively long times between cycles.

Fig. 4. shows the H_a vs. t curves for the activated MA 1h, MA 3h, MA 6h samples at 583k, 8bar H_2 . Before these curves were obtained, the hydrided sample was dehydrided for 2h at 583K under vacuum. The MA 6h sample has the highest hydriding rates as observed in Fig. 3.

Fig. 5 gives the H_a vs. t curves for the activated MA 6h sample at 583K under 7-11 bar H_2 . The curves exhibit two stages : the first stage with high hydriding rates, and the second stage with relatively low hydriding rates showing an "S" shape. During hydriding reaction, MgH_2 and Mg_2NiH_4 form (This will be shown by the X-ray diffraction pattern later). The hydriding rate of Mg_2Ni is reportedly much higher than that of Mg .^{18,19)} It is considered that in the first stage the Mg_2NiH_4 forms mainly and in the second stage MgH_2 forms.

Fig. 6. shows the H_a vs. t curves for the activated MA 6h sample under 9bar H_2 and at different temperatures. They show the curves similar to those in Fig. 5.

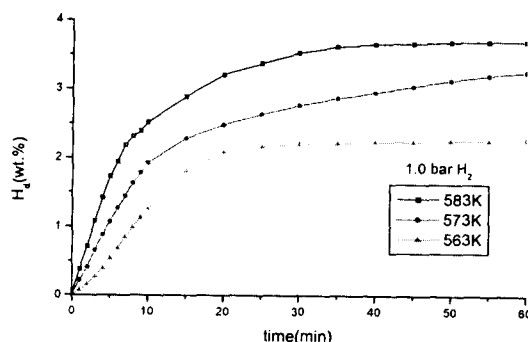


Fig. 8. H_d vs. t curves under 1.0 bar H_2 at different temperatures for the MA 6h sample.

The hydriding rate decreases as the temperature increases up to $H_a \cong 3\text{wt.}\%$, after which it increases as the temperature increases. It is reported that the hydriding rate of Mg_2Ni decreases as the temperature increases.¹⁸⁾ It is considered that the occurrence of the Mg_2Ni hydriding reaction in the beginning of the hydriding reaction brings about this behavior of the hydriding rate with the temperature.

H_d is defined as the weight percentage of desorbed hydrogen with respect to the sample weight.

Fig. 7 shows the H_d vs. t curves for the activated MA

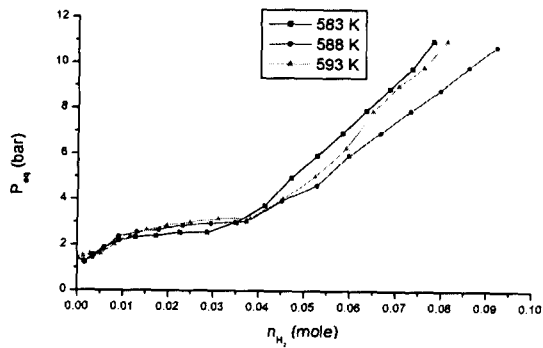


Fig. 9. Pressure-Composition Isotherms at different temperatures for the MA 6h sample.

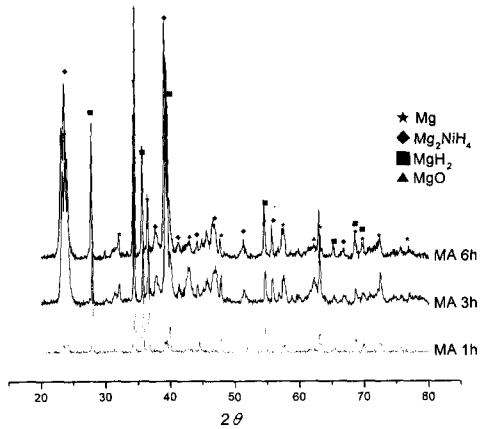


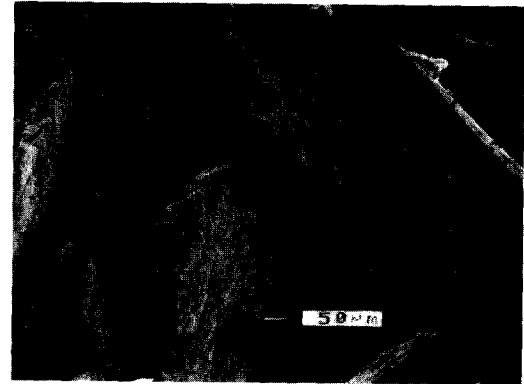
Fig. 10. X-ray diffraction patterns of the hydrided Mg-18wt.% Ni samples mechanically alloyed for three different times.

6h sample at 583K under 1.0-1.8bar H_2 . The H_d values increase monotonically from the beginning of the dehydriding reaction. The H_d value after 60min is 3.69wt.% at 583K under 1.0bar H_2 .

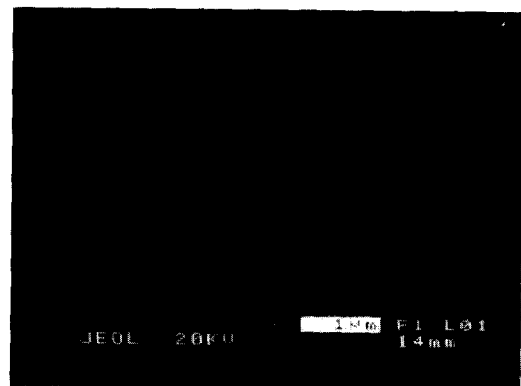
Fig. 8. shows the H_d vs. t curves for the activated MA 6h sample under 1.0bar H_2 at 563-583K. The hydriding rates under 1.0bar H_2 at 563K are relatively low.

Fig. 9. shows the pressure-composition isotherms at 583-593K for the MA 6h sample. Each isotherm exhibits one equilibrium plateau pressure; 2.53bar H_2 at 583K, 2.84bar H_2 at 588K and 2.99bar H_2 at 593K. These equilibrium plateau pressures correspond to those for the Mg- H_2 system.¹⁰⁾ We cannot see the equilibrium plateau pressures for the Mg_2Ni - H_2 system. It is considered that this results from the very small content of Mg_2Ni phase.

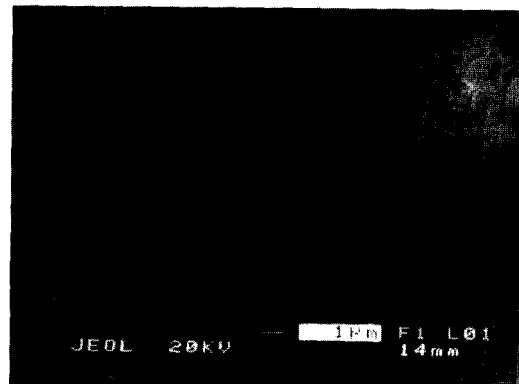
Fig. 10. exhibits the X-ray ($CuK\alpha$) powder diffraction patterns of the hydrided MA 1h, MA 3h, MA 6h samples. These samples were hydriding-dehydriding cycled after



(a)



(b)



(c)

Fig. 11. Microstructures of the MA 6h sample; (a) and (b) as prepared, and (c) after 51 hydriding-dehydriding cycles.

activation at 563-583K under 0-11bar H_2 . The MA 6h, MA 3h samples contains MgH_2 , Mg, Mg_2NiH_4 phases with a small quantity of MgO. The MA 1h sample has MgH_2 and Mg with a small quantity of Mg_2NiH_4 .

Fig. 11. shows the microstructures of the MA 6h sample; (a) and (b) as prepared, and (c) after 51 hydriding-dehydriding cycles. The particles of the MA

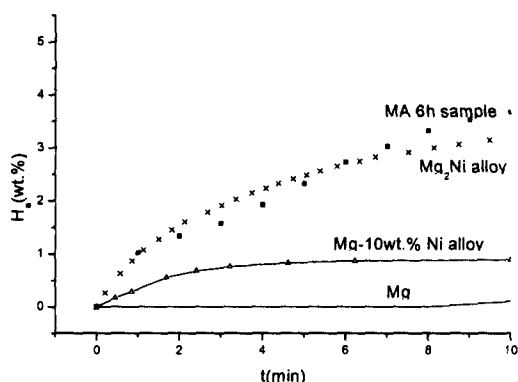


Fig. 12. Hydriding curves of the MA 6h sample, the Mg-10wt.%Ni alloy, the pure Mg, and the Mg₂Ni alloy.

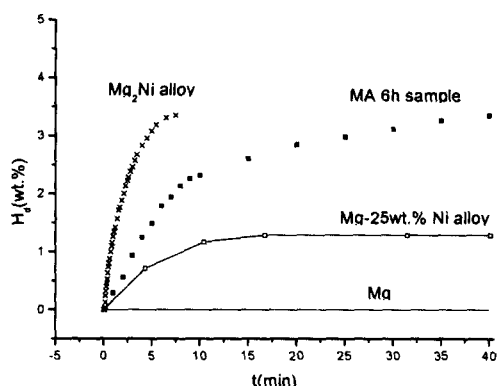


Fig. 13. Dehydriding curves of the MA 6h sample, the Mg-25wt.%Ni alloy, the pure Mg, and the Mg₂Ni alloy.

6h sample as prepared have the shape like an elliptical plate with irregular surface. After hydriding-dehydriding cycling, the particles become small aggregates which are made up of very tiny spherical particles.

Fig. 12. gives the hydriding curve of the MA 6h sample at 583K 8bar H₂, with those of the Mg-10wt.%Ni alloy at 582K 9bar H₂,¹⁷⁾ the pure Mg at 675K 30bar H₂,¹⁹⁾ and the Mg₂Ni alloy at 573K 7bar H₂¹⁸⁾ reported earlier. The MA 6h sample has higher hydriding rate than the pure Mg and the Mg-10wt.%Ni alloy, and a little lower hydriding rate than the Mg₂Ni alloy. The MA 6h sample has the largest hydrogen-storage capacity.

Fig. 13. shows the dehydriding curves of the MA 6h sample at 583K 1.4bar H₂, together with those of the Mg-25wt.%Ni alloy at 618K under vacuum,⁴⁾ the pure Mg at 595K 1.5bar H₂,²⁰⁾ and the Mg₂Ni alloy at 576K 1.4bar H₂²¹⁾ reported earlier. The Mg₂Ni alloy has the highest dehydriding rate. The MA 6h sample exhibits

much higher hydriding rates than the pure Mg and the Mg-25wt.%Ni alloy.

The mechanical alloying of Mg with Ni and the hydriding-dehydriding cycling increase the hydriding and dehydriding rates by facilitating nucleation (by creating defects on the surface of the Mg particle and by the additive) and by shortening the diffusion distances (by reducing the particle size of Mg). These effects lead to the above results that the hydriding and dehydriding rates of Mg-18wt.%Ni are higher than those of the pure Mg, the Mg-10wt.%Ni alloy and the Mg-25wt.%Ni alloy.

4. Conclusions

The hydriding and dehydriding properties of a mechanically-alloyed mixture with a composition Mg-18wt.%Ni were investigated and the following conclusions were drawn:

Among the mixtures mechanically alloyed for 1h, 3h, and 6h, the mixture mechanically alloyed for 6h (MA 6h sample) shows the best properties of activation, hydriding and dehydriding.

The Mg₂Ni phase forms in the mechanically-alloyed Mg-18wt.%Ni mixture along with hydriding-dehydriding cycling.

The MA 6h sample is relatively easily activated and has higher hydriding rate than the pure Mg, the Mg-10wt.%Ni alloy and a little lower hydriding rate than the Mg₂Ni alloy.

The MA 6h sample shows lower dehydriding rate than the Mg₂Ni alloy but higher dehydriding rate than the pure Mg and the Mg-25wt.%Ni alloy.

The MA 6h sample has larger hydrogen-storage capacity than the pure Mg and the other alloys.

Acknowledgement

The authors wish to acknowledge the financial support of the Korea Research Foundation made in the program year of 1998.

References

1. Vose, "Metal Hydrides", U.S. Patent 2 944, p.587 (1961).
2. J.J. Reilly and R.H. Wiswall, *Inorg.Chem.*, **6**(12), 2220 (1967).
3. J.J. Reilly and R.H. Wiswall Jr, *Inorg. Chem.*, **7**(11), 2254 (1968).
4. D.L. Douglass, *Metall. Trans. A*, **6**, 2179 (1975).
5. D.L. Douglass, in A.F. Anderson and A.J. Maeland (eds.), "Hydrides for Energy Storage", Proceedings

- International Symposium, Geilo, Norway, August 1977, pp.151-184.
6. M.H. Mintz, Z. Gavra and Z. Hadari, *J. Inorg. Nucl. Chem.*, **40**, 765 (1978).
 7. M. Pezat, A. Hbika, B. Darriet and P. Hagenmuller, French Anvar Patent 78 203 82, 1978. *Mater. res. Bull.*, **14**, 377 (1979).
 8. M. Pezat, B. Darriet and P. Hagenmuller, *J. Less-Common Met.*, **74**, 427 (1980).
 9. Q. Wang, J. Wu, M. Au and L. Zhang, in "Hydrogen Energy Progress V", Proceedings 5th World Hydrogen Energy Conference, Toronto, Canada, July 1984. vol.3, edited by T. N. Veziroglu and J.B. Taylor (Pergamon, New York) pp.1279-1290.
 10. B. Tanguy, J.L. Soubeyroux, M. Pezat, J. Portier and P. Hagenmuller, *Mater. Res. Bull.*, **11**, 1441 (1976).
 11. F.G. Eisenberg, D.A. Zagnoli and J.J. Sheridan III, *J. Less-Common Met.*, **74**, 323 (1980).
 12. B. Bogdanovic, *Int. J. Hydrogen Energy*, **9(11)**, 937 (1984).
 13. E. Akiba, K. Nomura and S. Ono and S. Suda, *Int. J. Hydrogen Energy*, **7(10)**, 787 (1982).
 14. E. Akiba, K. Nomura and S. Ono, *J. Less-Common Met.*, **89**, 145 (1983).
 15. J.M. Boulet and N. Gerard, *J. Less-Common Met.*, **89**, 151 (1983).
 16. S. Ono, Y. Ishido, E. Akiba, K. Jindo, Y. Sawada, I. Kitagawa and T. Kakutani, in "Hydrogen Energy Progress V", Proceedings 5th World Hydrogen Energy Conference, Toronto, Canada, July 1984, Vol. 3, edited by T.N. Veziroglu and J.B. Taylor (Pergamon, New York) pp. 1291-1302.
 17. J.M. Boulet, thesis of 3^{ème} cycle, Université de Dijon (France), 1982.
 18. M.Y. Song, M. Pezat, B. Darriet, J.Y. Lee and P. Hagenmuller, *J. Mater. Sci.*, **21**, 346 (1986).
 19. A.S. Pedersen, J. Kjølner, B. Larsen and B. Vigeholm, in "Hydrogen Energy Progress V", Proceedings 5th world Hydrogen Energy Conference, Toronto, Canada, July 1984. vol.3, edited by T.N. Veziroglu and J.B. Taylor (Pergamon, New York) pp.1269-1277.
 20. B. Vigeholm, J. Kjølner, B. Larsen and A. Schrøder Pedersen, *Int. J. Hydrogen Energy*, **8(10)**, 809 (1983).
 21. M.Y. Song, B. Darriet, M. Pezat, J.Y. Lee and P. Hagenmuller, *J. Less-common Met.*, **118**, 235 (1986).